

WHEEL/RAIL FRICTION POWER IN CURVED TRACK

Andrei TUDOR¹, Nicolae SANDU² Elias TOUNTAS³

Lucrarea își propune să analizeze alunecările rigide longitudinale, laterale și de spin și puterea consumată prin frecare la contactul sănă – roată, pentru cazul unui traseu în curbă. Se exemplifică forma și geometria suprafeței de contact pentru cazul săinei UIC 49 și roții S78. Se deduce ca pentru cazul analizat (S78-UIC49), contactul poate fi elliptic și liniar, funcție de poziția roții pe sănă. Modelul teoretic permite analiza pierderilor de putere prin frecare ca funcție de principali parametri ai roții și ai săinei: raza curbei, jocul roții pe sănă, unghiul de atac, viteza de rostogolire, viteza unghiulară de spin, raza roții. Pierderile de putere prin frecare constituie date de intrare pentru modelarea procesului de uzare a roții și a săinei.

The paper analyses the longitudinal, lateral and spine creepages and the friction power for the wheel-rail contact on curved track. The geometry of UIC49 rail and S78 wheel and their contact are shown as an example. The contact area can be of elliptic or rectangular form, as a function to the wheel position relative to rail. The theoretical model can compute the friction power as a function to the main wheel – rail parameters: curved track radius, clearance between wheel and rail, yaw angle, rolling velocity, angular spin velocity and nominal radius of wheel. The friction power can be used that input parameters for the rail wear model and the wheel wear model.

Keywords: Adhesion; creepage; traction; friction power; curved track.

1. Introduction

The simplest theory of rolling is the one in which wheel and rail are considered as rigid and the contact is governed by Coulomb friction law. In such a theory, the circumferential velocity of the wheel and the translational velocity of the wheel over the rail are equal unless the tangential force is saturated. Since the contact takes place on a single point, the transmitted forces are concentrated forces.

The first theory of the continuum rolling contact started in 1926 when Carter published the paper “On the action of locomotive driving wheel” [1]. In

¹ Prof., Univesity POLITEHNICA of Bucharest, Romania, e-mail: tudor@meca.omtr.pub.ro

² Eng., Romanian Authority of Rail Way, Bucharest, Romania

³ Eng., ATTIKO METRO A.E. Athena, Greece

in this theory the wheel is approximated by a cylinder and rail by an infinite half-space.

Carter showed that the difference between the circumferential velocity of a driven wheel and the translational velocity of the wheel over the rail has non-zero value as soon as an accelerating or braking couple is applied to the wheel; this difference increases in absolute value with increasing couple until the Coulomb maximum value is reached. The law (the creepage-force law) connecting the driving-braking couple and velocity difference.

Around 1956, de Pater and Johnson were active in the field of three-dimensional theory of continuum rolling contact [2]. They established that the Hertz solution can be used to predict the shape and size of contact area and the normal pressure carried by it. It turns out that the contact area is elliptic in form, with semiaxes a and b in the rolling and lateral direction respectively. The ratio of the axes, a/b , depends only on the curvatures of wheel and rail. The size of contact depends on the normal force F_z , but it is independent of the tangential force F_t .

De Pater and Johnson analysed the motion of the wheel with respect to the rail when both are considered as rigid: that is, they sought for the generalization of Carter's notion of creepage.

Kalker generalized the linear theory to the case where the relative rigid slip is small, the contact area is hertzian elliptic and rolling takes place in the direction of one of the axes of the contact ellipse.

To define the friction energy in wheel-rail contact, it is necessary to know the longitudinal, lateral and spin creepage and the creepage - force law.

In the present paper, we propose a model to define the contact area and the friction power for a wheelset on the curved track of metro, when the linear Kalker's theory of creepage is used.

2. Contact geometry of wheel-rail contact in curved track

The question of adhesion always arises when discussing the increase of the speed of service in conventional wheel-rail systems. The increased acceleration and deceleration efforts of the vehicle needed for the increase in speed are limited by the adhesion force between wheel and rail. Friction conditions between wheel and rail play important roles in car dynamic behaviour because the forces generated by contact of wheel and rail depend on the friction (or creep force) characteristics [3], [4], [5].

In a wheel/rail contact, both rolling and sliding occur in the contact area. On a straight track, the wheel tread is in contact with the rail head, but in curves the wheel flange may be in contact with the gauge corner of the rail.

The standard geometry of wheel and rail is realized by computer simulation, as an example in Fig.1 for the right rail-wheel. These geometries are valuable for the UIC 49 rail profile- STAS 2953-80 and S78 wheel profile- STAS 112/3-90 and correspond to functionality position for the rectilinear direction of the train.

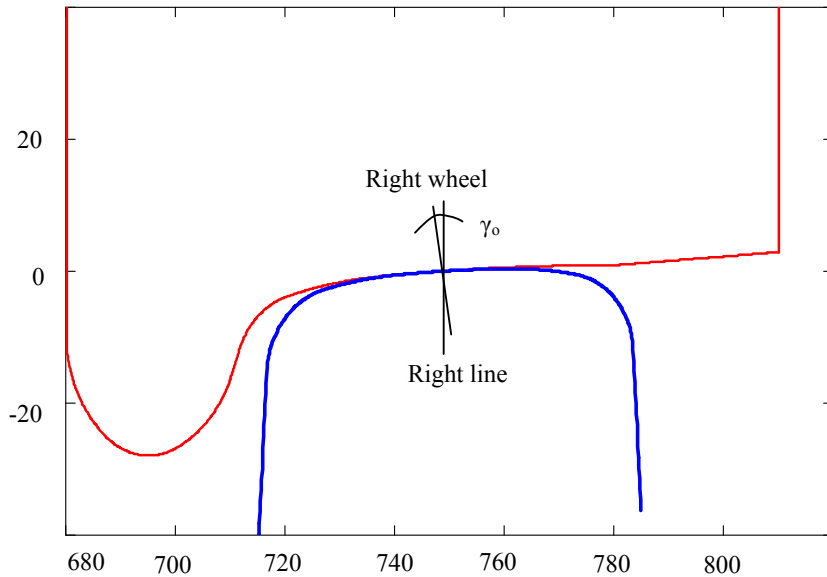


Fig.1. The standard geometry of S75 wheel profile and UIC 49 rail profile.

It is known that the rails are inclined with the angle $\gamma_0 = \text{atan}(1/20)$ with respect to the horizontal direction.

The contact area and the normal pressure are defined by the famous Hertz solution. The contact area is elliptic in form, with semiaxes a and b in the rolling and lateral direction respectively. The ratio of the axes, a/b , depends only on the curvatures of wheel and rail.

To use the hertz solution, we developed a computer program for all point contact between wheel and rail. The ratio of the axes, a/b , is named the elliptic parameter. This parameter has an aspect as shown in Fig. 2, for the S78 wheel and the UIC 45 rail and three values of yaw angle (α).

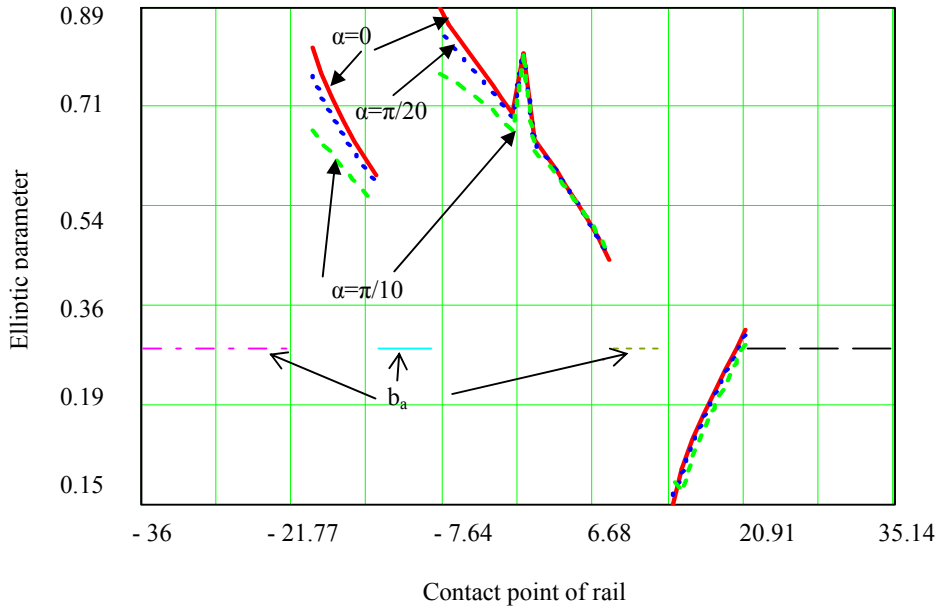


Fig. 2. Elliptic factor of S78 wheel and UIC 45 rail contact.

It can be see that for some points of wheel-rail contact, the total curvature contact is nearly to zero, and the hertzian theory will be applicable for linear contact. Thus, the contact between wheel and rail is linear when the wheel is situated in the following intervals: (-36, -21.49), (8.51, 13.65) and (21.148, 36). The contact length and the average radius of wheel for these intervals are respectively: $L_1 = 22.343$ mm, $R_1 = 443.647$ mm, $L_2 = 5.146$ mm, $R_2 = 439.64$ and $L_3 = 22.343$ mm, $R_3 = 439.429$ mm, for the nominal diameter of wheel $D_w = 880$ mm. To compare the hertzian linear contact with the hertzian elliptic contact, we define the equivalent dimensionless parameter b_a

$$b_a = \frac{b_{Hl}^2 L}{a_{He}^3} \quad (1)$$

where $2b_{Hl}$ is the hertzian length of wheel-rail contact; a_{He} - hertzian semiaxle in rolling direction for the central contact point ; L- contact length. The equivalent dimensionless parameter b_a is presented in the fig. 2

Fig. 3 shows the form of contact area between the S78 wheel and the UIC 49 rail.

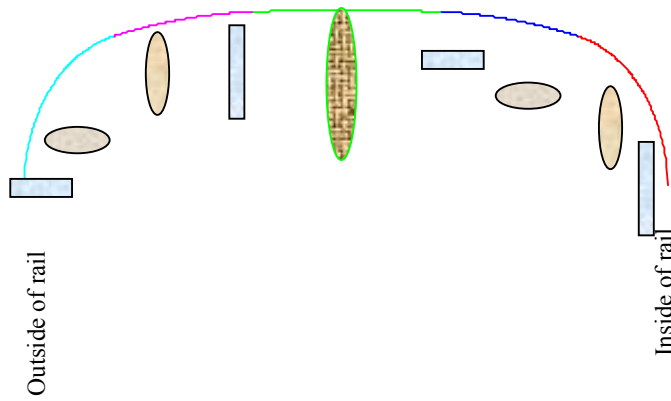


Fig.3. Elliptic and linear contact of wheel- left line.

3. The creepages of wheel-rail contact in curved track

To define the creepage, we consider a wheelset on a track (Fig. 4 (a)). The wheel makes a yaw angle α with the rail. The yaw angle α has an angular velocity α_v . The wheelset moves in lateral direction y with a velocity v_y , a translational velocity v_T , and a circumferential velocity v_C . The angular velocity of the wheel set is Ω . We define that $y > 0$ when the wheelset shifts towards the left side of track and the yaw angle $\alpha > 0$ if it is inclined, in the clockwise direction, between the axis of wheelset and the lateral direction of track pointing to the left side.

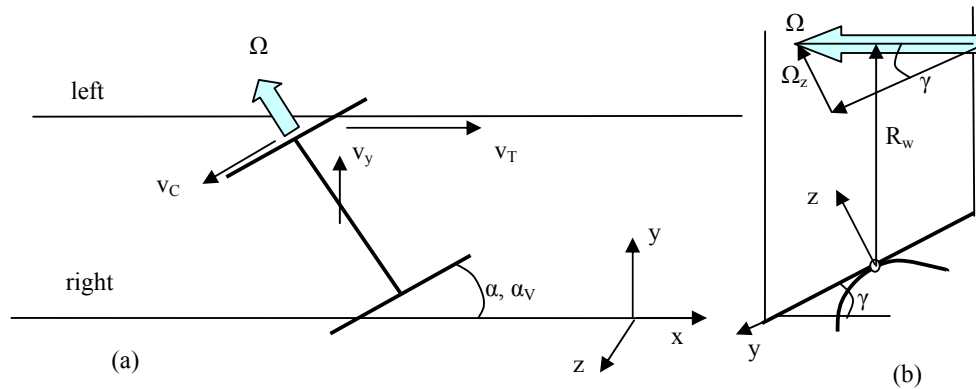


Fig.4. The creepage: (a) a wheelset on a track; (b) illustration of a camber spin [1].

Longitudinal creepage (ξ) arise *inter alia* through the difference in effective rolling radii of the wheels, left and right, due to conicity; also through accelerating or braking couples and, very important, through the rotation velocity α_v of the yaw angle α , by which the left wheel moves with a different velocity over the rail than the right wheel.

The velocities v_T and v_C make an angle α one to another. Hence the difference velocity $v_T - v_C$ has a component in the y direction; velocity v_y also gives rise to *lateral creepage* (η).

The spin creepage (Φ) consists of two parts. The first part is due to the velocity of the yaw angle, α_v ; the second is a consequence of conicity. The spin creepage due to conicity is called *camber* in the automotive industry and is illustrated in Fig. 4(b).

As shown in Fig. 5, in the section of sharp curve the leading wheelset in a bogie displacement laterally from track center and has a large yaw angle, but the trailing wheelset in the same bogie has almost no lateral displacement and yaw angle. For this reason, large longitudinal creep rate (about 2 %) in trailing wheelset can be produced as the difference of rail length inside and outside cannot be absorbed.

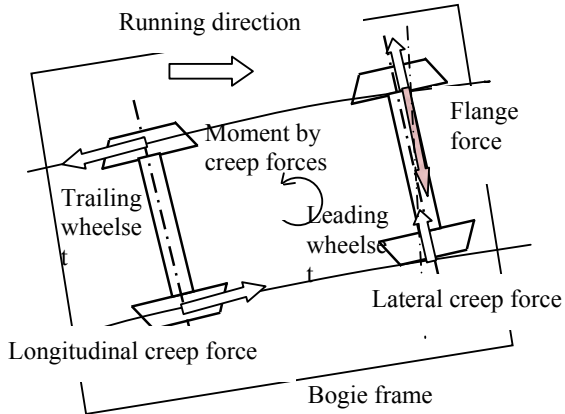


Fig.5. Bogie attitude and contact force in curving.

The contact parameters depend on the profiles of the wheel and rail (yaw angle of wheelset, α , lateral shift of wheelset, y , with respect to the centre line of track) and the radius of curves R .

When two successive wheelset are situated in curved track, a possibility to adapt to the line is necessary. In this case, the yaw angle varies in the interval α_c and α_s

$$\alpha_c = a \sin\left(\frac{a_p}{2R}\right) \quad \alpha_s = a \sin\left(\frac{a_p^2 + 2Ry - y^2}{2Ra_p}\right) \quad (2)$$

where a_p is the distance between two successive rigid wheelset.

The longitudinal creepage can be writing as a generalisation of Jin, Wu and Wen equations [6]:

- for the left line curve

$$\xi_{lc} = \left(1 - \frac{r + \gamma y_c}{r}\right) \cos(\alpha_s) + \frac{1}{r} \left[(y_c + e_c) \cos\left(\frac{vt}{r}\right) - (r + \gamma y_c) \sin\left(\frac{vt}{r}\right) \right] \frac{r\alpha_v}{v} \quad (3)$$

where r is the radius of the nominal rolling circle of wheel (mm), γ - contact angle (rad), y_c -distance from nominal rolling circle of wheel to instant rolling circle (mm), e_c - distance from center of wheelset to nominal rolling circle of wheel (mm), v - forward speed of wheelset, t - time, α_v - yaw angle velocity of wheelset (rad/s);

-for the right rail curve

$$\xi_{rc} = \left(1 - \frac{r - \gamma y_c}{r}\right) \cos(\alpha_s) + \frac{1}{r} \left[(y_c - e_c) \cos\left(\frac{vt}{r}\right) - (r - \gamma y_c) \sin\left(\frac{vt}{r}\right) \right] \frac{r\alpha_v}{v} \quad (4)$$

The tangential creepage:

- for the left rail curve

$$\eta_{lc} = -\sin(\alpha_s) \cos\left(\frac{vt}{r} + \gamma\right) + \left[\begin{array}{l} \cos(\alpha_s) \cos\left(\frac{vt}{r} + \gamma\right) + \left[-y_{cv} + (r + \gamma y_c) \frac{vt}{r} \cos(\gamma) \right] \cos(\gamma) + \\ + \left[(e_c - y_c) \frac{vt}{r} \cos(\gamma) - \gamma \right] \sin(\gamma) \end{array} \right] \frac{y_{cv}}{v} \quad (5)$$

where y_{cv} is the lateral velocity of wheelset center (mm);

- for the right rail curve

$$\eta_{rc} = -\sin(\alpha_s) \cos\left(\frac{vt}{r} - \gamma\right) + \left[\begin{array}{l} \cos(\alpha_s) \cos\left(\frac{vt}{r} - \gamma\right) + \left[-y_{cv} + (r - \gamma y_c) \frac{vt}{r} \cos(\gamma) \right] \cos(\gamma) + \\ + \left[(e_c + y_c) \frac{vt}{r} \cos(\gamma) + \gamma \right] \sin(\gamma) \end{array} \right] \frac{y_{cv}}{v} \quad (6)$$

The spin creepage:

-for the left rail curve

$$\phi_l = \frac{-\sin(\gamma)}{r} + \frac{1}{r} \cos\left(\gamma + \frac{vt}{r}\right) \frac{r\alpha_v}{v} \quad (7)$$

-for the right rail curve

$$\phi_r = \frac{\sin(\gamma)}{r} + \frac{1}{r} \cos\left(\gamma - \frac{vt}{r}\right) \frac{r\alpha_v}{v} \quad (8)$$

We consider that relative motion of wheel and rail is the rigid slip and the wheel has a translation and a rotation about the common normal at the centre of contact area, which is taken as the z axis. The dimensionless traction force in rolling (longitudinal) direction, F_{ax} , and lateral direction, F_{ay} , and the dimensionless moment spin, M_{az} , can be written with Kalker's theory. Thus,

$$F_{ax} = \frac{F_x}{a^2 G} = -\frac{1}{e_e} C_{11} \xi, \quad (9)$$

where F_x is the traction force in longitudinal direction; a- semi axis of contact ellipse length in rolling direction; G- equivalent modulus of rigidity; e_e – ellipticity factor of contact ellipse (b/a or $a/b < 1$, b –semi axe of contact ellipse length in lateral direction);

$$F_{ay} = \frac{F_y}{a^2 G} = -\frac{1}{e_e} C_{22} \xi - \frac{a}{e_e^{3/2}} \phi, \quad (10)$$

$$M_{az} = \frac{M_z}{a^3 G} = -\frac{1}{e_e^{3/2}} C_{32} \eta - \frac{a}{e_e^{3/2}} C_{33} \phi \quad (11)$$

where C_{11} , C_{22} , C_{32} and C_{33} are Kalker's coefficients, which depend on the eccentricity of ellipse contact e_e and Poisson's ratio, ν :

$$C_{11}(e_e) = \frac{-\pi}{B(e_e) - \nu [D(e_e) - C(e_e)]}; \quad C_{22}(e_e) = \frac{-\pi}{B(e_e) - \nu e_e^2 C(e_e)}$$

$$C_{32}(e_e) = -\frac{C_{22}(e_e) \sqrt{e_e}}{3}; \quad C_{33}(e_e) = \frac{\pi}{4} \left[1 - \frac{\nu(\Lambda(e_e) - 2)}{(1-\nu)\Lambda(e_e) - 2 + 4\nu} \right]$$

where $B(e_e)$, $C(e_e)$ and $D(e_e)$ are integral functions with the e_e argument:

$$B(e_e) = \int_0^{\pi/2} \cos^2 x (\cos^2 x + e_e^2 \sin^2 x)^{-1/2} dx; \quad C(e_e) = \int_0^{\pi/2} (\cos^2 x + e_e^2 \sin^2 x)^{-3/2} dx$$

$$D(e_e) = \int_0^{\pi/2} \left(\cos^2 x + e_e^2 \sin^2 x \right)^{-1/2} dx.$$

We define the function $\Lambda(e_e)$, thus that C_{33} coefficient has the same value for $a/b = 1$ and $b/a = 1$:

$$\Lambda(e_e) = \frac{(2-4\nu)\pi - 8(1-3\nu)(1-\nu)e_e}{\pi(1-\nu) - 4(1-\nu)(1-2\nu)e_e}.$$

The dimensionless traction forces and spin moment (9-11 equations) can be evaluated for the left and right direction with the creepage coefficients (3- 8 equations).

4. The friction power of wheel-rail contact in curved track

In the curved track it is possible all types of creepage are possible. Thus, evaluated the friction power for each contact point between wheel and rail can be. The effect of friction is the temperature field and the wear of wheel and rail. We consider that the origin of friction is the sliding zone of ellipse or linear contact, so the total dimensionless friction power can be written as

$$P_{af} = \frac{P_f}{a^2 G v_r} = F_{ax} \xi + F_{ay} \eta \frac{y_{cv}}{v_r} + a M_{az} \phi \quad (12)$$

This equation must be applied for the left and right lines, by used the creepage coefficients, which are indicated by equations (9-11). This friction power is dissipated by elliptic or linear contact and it is possibility to define the specific friction power. The wear of wheel or rail depends on the specific friction power as an input parameter. The dimensionless specific friction power can be evaluated by the equation

$$P_{afs} = \frac{P_f}{\pi a^2 e_e G v_r} = \frac{P_{af}}{\pi e_e} \quad (13)$$

Further, we show some numerical results, in which the effects of wheel-rail contact on the friction power are taken into consideration.

The analytical results are obtained by the geometrical parameters of wheel-rail from metro in Bucharest and partial from metro in Athens. To obtain the effect of some geometrical parameters, we consider the following values: radius of the nominal rolling circle of wheel $r_o = 0.4 \text{ m}$, the lateral shift of wheelset with respect to the center line of track $y_c = 1 \text{ mm}$, the distance between two successive rigid wheelset $a_p = 2 \text{ m}$, the curved track radius $R = 200 \text{ m}$ and $R = 400 \text{ m}$, the clearance between wheel and curved line $\sigma = 9 \text{ mm}$, the yaw angle velocity

of wheelset $\alpha_v = 0.1 \text{ rad/s}$, the rolling velocity of wheelset $v = 36 \text{ km/h}$, the lateral velocity of wheelset center $y_{cv} = 0.3 \text{ m/s}$, the ellipticity of contact area $e_e = 0.2$ and the contact semi axis in rolling direction $a = 3 \text{ mm}$.

Fig. 6 shows the dimensionless specific friction power versus time, for the wheel-left rail.

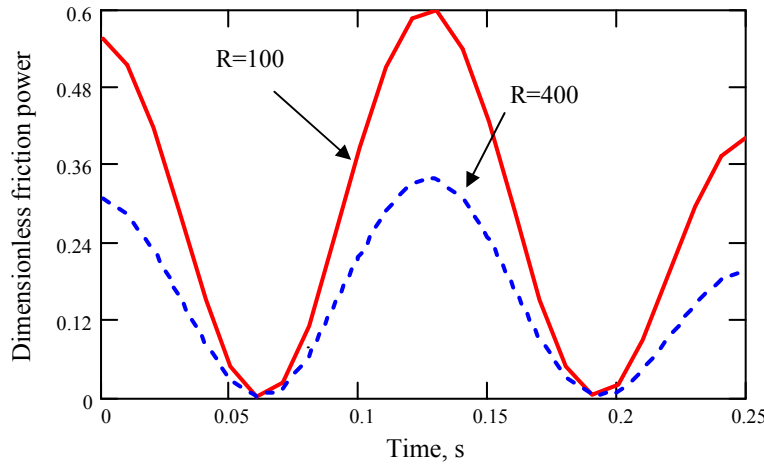


Fig. 6. Friction power v.s. rolling time.

The effect of rolling velocity on the dimensionless friction power is shown in the Fig. 7, for the rolling time $t = 0.1 \text{ s}$. One can see that the friction power decreases with the rolling velocity and the radius of curved track.

Fig. 8 shows the friction power of wheel-left line, P_{afl} , and wheel-right line, P_{afr} , for two radii of curved track, as a function of lateral displacement.

The effect of curved track radius is analysed in Fig. 9, for the three rolling velocities, which are characteristic for the metro. It can be observed that the friction power decreases when the radius of line and rolling velocity increase.

The friction power increases rapidly, when the clearance between wheel and line is greater, as shown in the Fig. 10.

Fig. 11 shows the effect of nominal wheel radius on the friction power for the left wheel-rail (P_{afl}) and right wheel-rail (P_{afr}), when the rolling velocity is 36 km/h, respectively 54 km/h.

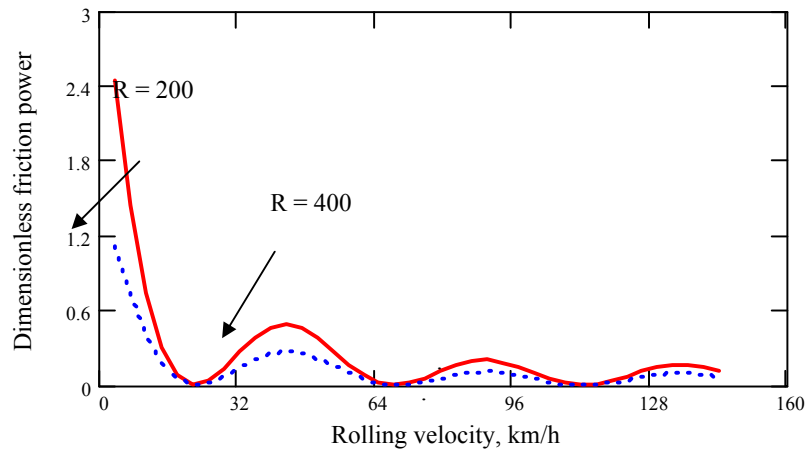


Fig. 7. Friction power vs rolling velocity.

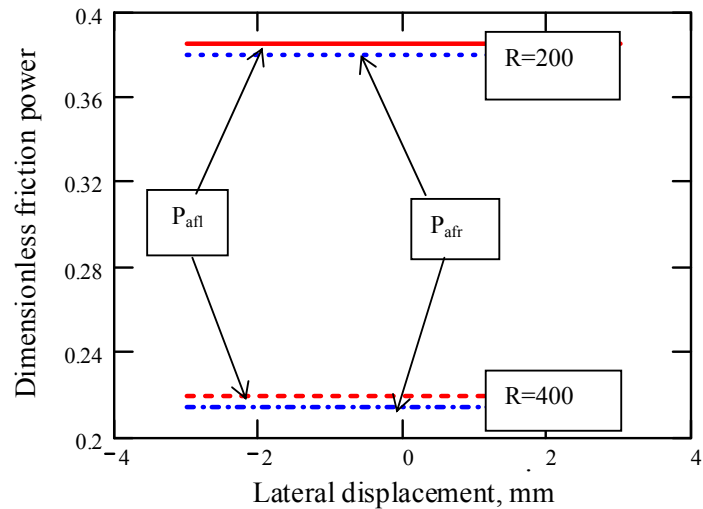


Fig. 8. Friction power v.s. lateral displacement.

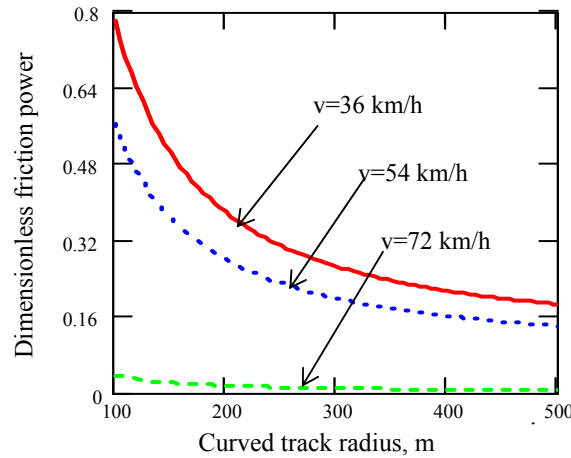


Fig. 9. Friction power v.s. curved track radius.

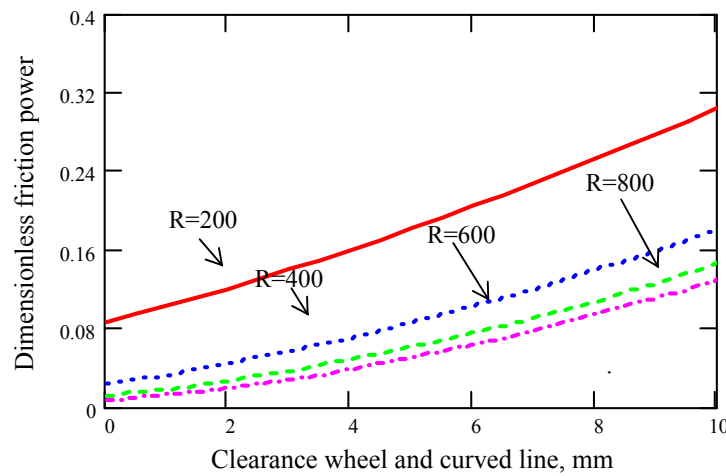


Fig. 10. Friction power v.s. clearance in curved track.

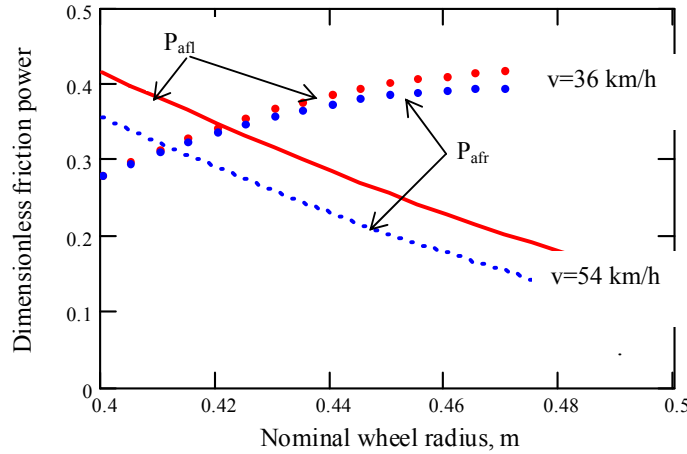


Fig. 11. Friction power v.s. nominal wheel radius.

From the results described in Figs. 6-11 we know that the effects of geometrical parameters of wheelset and track on the friction power are very large.

The adhesion force between rail and wheel is an essential factor for high-speed railway systems, especially in braking, as deceleration for stopping the train within the specified distance is not obtained if the needed adhesion force can not be assured. Moreover, most of surface damages on wheel-treads such as flats, skidding marks and shelling will occur to give rise to noise and vibration of vehicle and deteriorate the riding quality. For these reasons, the technique to control adhesion force makes an important and fundamental research subject inherent to railways.

5. Conclusions

Based on the theoretical work, the following can be concluded:

- Under the condition of the S 78 wheel and the UIC 49 rail, the contact area can be elliptic or linear, as a function of the position of wheelset in track.
- The elliptic parameter has some values and the elliptic contact can be transformed into linear hertzian contact.
- To use the Kalker's coefficient for creepage, it is necessary continuity and linear interpolation, when the ratio of elliptic axe is smaller or greater to unity.
- The total friction power of wheel-rail in curved track is proportional to the longitudinal creep, the lateral creep and the spin creep.

- e) The friction power decreases with the rolling velocity and the radius of curved track.
- f) The friction power increases with the clearance between wheel and rail and the nominal radius of wheel.
- g) The friction power is different for the left wheel-contact and the right-contact.

R E F E R E N C E S

- [1] *J.J. Kalker*, "Wheel-rail rolling contact theory" *Wear* **144** (1991), 243-261.
- [2] *K.L. Johnson*, Contact mechanics. Cambridge University Press 1985.
- [3] *H. Chen, T. Ban, M. Ishida, T. Nakahara*, Adhesion between rail/wheel under water lubricated contact, *Wear* **253** (2002), 75-81.
- [4] *T. Ohyama*, Tribological studies on adhesion phenomena between wheel and rail at higher speed, *Wear* **144** (1991), 263-275.
- [5] *H. Harrison, T. McCanney, J. Cotter*, Recent developments in coefficient of friction measurements at the rail/wheel interface, *Wear* **253** (2002), 114-123.
- [6] *W. Zhang, J. Chen, X. Wu, X. Jin*, Wheel/rail adhesion and analysis by using full scale roller rig, *Wear* **253** (2002), 82-88.
- [7] *X. Jin, P. Wu, Z. Wen*, Effects of structure elastic deformations of wheelset and track on creep forces of wheel/rail in rolling contact, *Wear* **253** (2002), 247-256.